Journal of
Mechanical
Science and
Technology

Journal of Mechanical Science and Technology 21 (2007) 448~454

An Experimental Analysis of the Effect of Wind Load on the Stability of a Container Crane

Seong Wook Lee[a], Jae Joon Shim[b], Dong Seop Han[c], Geun Jo Han[d], Kwon Soon Lee[e,*]

[a]Department of Mechanical Engineering, Dong-A University, 840, Hadan2-Dong, Saha-gu, Busan, 604-714, Korea
[b]School of Automobile & Machine, B.I.T., Mt 48-6, Gopo3-Dong, Buk-gu, Busan, 616-737, Korea
[c]Department of Mechanical Engineering, Dong-A University, 840, Hadan2-Dong, Saha-gu, Busan, 604-714, Korea
[d]Department of Mechanical Engineering, Dong-A University, 840, Hadan2-Dong, Saha-gu, Busan, 604-714, Korea
[e]Department of Electrical Engineering, Dong-A University, National Research Laboratory (NRL), 840, Hadan2-Dong, Saha-gu, Busan, 604-714, Korea

(Manuscript Received March 27, 2006; Revised December 15, 2006; Accepted December 22, 2006)

Abstract

This study was conducted to analyze the effects of wind loads on the stability of a 50-ton container crane using wind tunnel testing. The experiments were performed in order to furnish designers with data that can be used in the design of a container crane that is wind resistant, assuming an applied wind load of 75 m/s velocity. Data acquisition conditions for this experiment were established in accordance with similarity to a reduced-scale model. The scale of the container crane model, wind speed and time were selected as 1/200, 1/13.3, and 1/15, respectively, and the experiment was conducted using an Eiffel type atmospheric boundary-layer wind tunnel having a 11.52 m^2 cross-sectional area. All directional drag and overturning moment coefficients were investigated and uplift forces due to wind load at each supporting point were analyzed.

Keywords: Container crane, Wind tunnel test, Drag coefficient, Overturning moment coefficient, Structural stability

1. Introduction

Container cranes are vulnerable to difficult weather conditions because there is no shielding facility to protect them from high winds. Container cranes in current use can reach a maximum height of 100 m in the stowed mode (i.e. when the boom has been raised). Therefore, they may easily be affected by wind loads, demonstrated especially in the case of the sudden onset of the typhoon "Maemi," during which a total of 11 container cranes were damaged due to heavy wind loads, causing heavy losses for the Korean logistics sector. Therefore, wind loads can be considered as the most important factor under any load conditions for container crane design. For example, wind loads are not only applied to analyze the structural strength of each part of a container crane, but also in the design of stowing devices (tie-downs, stowage pins and rail clamps, etc.) to prevent container cranes from overturning (e.g. Han et al., 2004).

To calculate accurately the wind loads applied to a container crane, a basic design test and a wind tunnel test must be performed. These tests are divided into two stages by Korean container crane manufacturers. The basic design test is performed in house using the 'BS2573' standard. However, for the wind tunnel test, data provided by a foreign consultative committee are used. Unfortunately, this practice causes a container crane to reduce the structural reliability, because the

*Corresponding author. Tel.: +82 51 200 7739; Fax.: +82 51 200 7743
E-mail address: kslee@dau.ac.kr

wind tunnel test model parameters established by the foreign consultative committee are different from those required for domestically produced container cranes.

Therefore, container crane designers should be provided with wind tunnel test results for domestically produced models in order to enable the design and implementation of wind-resistant container cranes more suitable for Korean weather conditions. Consequently, in this study we aim to analyze the effects of wind loads according to the changes in wind direction and machinery house locations on the structural stability of 50-ton container cranes of a type of berth widely used in Korea using a wind tunnel test.

2. Wind tunnel test

2.1 Design of wind velocity and wind characteristics

In this study, the wind tunnel test was performed based on the assumption that a wind load of 75 m/s velocity is applied to a container crane. Mean wind velocity according to height was conformed to *Design Criteria of a Road Bridge* (Ministry of Construction & Transportation of the Korean Government, 2000) and turbulence intensity and wind velocity spectrum was conformed *Load Criteria of Building Structures* (Ministry of Construction & Transportation of the Korean Government, 2000). Because a container crane is generally installed on a shoreline, the terrain roughness category was selected to be Exposure I (*Design Criteria of a Road Bridge*) and Exposure D (*Load Criteria of Building Structures*) in the boundary layer for the wind tunnel test. Fig. 1 illustrates the vertical distribution of mean wind velocity and turbulence intensity, and the wind velocity spectrum at a height of 64 m (32 cm in wind tunnel test model), which is the apex beam location of the container crane shown in Fig. 2.

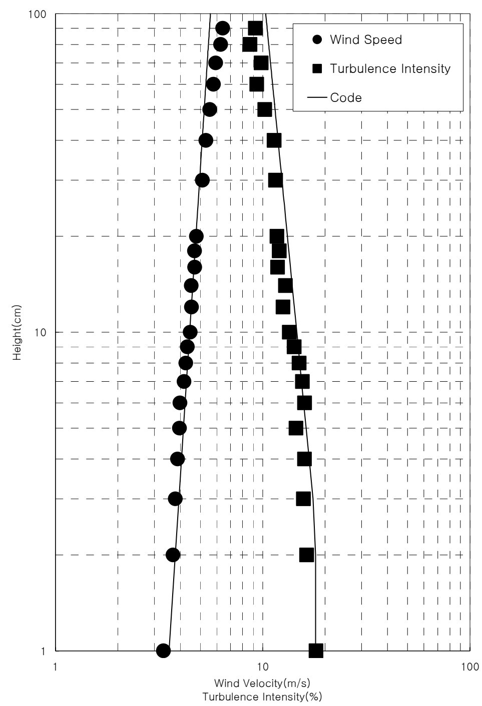

Fig. 1. Wind velocity and turbulence intensity according to height.

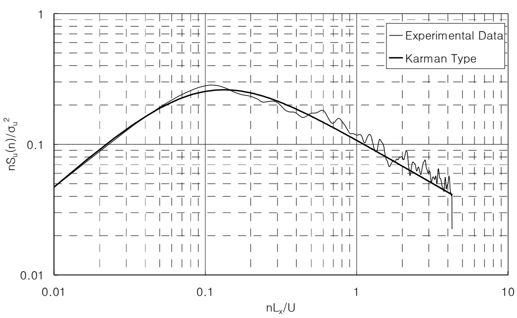

Fig. 2. Wind velocity spectrum at 32 cm height in the wind tunnel.

2.2 Experimental facilities and measuring equipments

The wind tunnel used for measuring the wind load is an Eiffel-type atmospheric boundary-layer wind tunnel at the Hyundai Institute of Construction Technology. The total length is 53 m, and the dimensions of the measuring part are 4.5 m (width)×2.5 m (height)×25 m (length). The wind velocity range is 0.3~17.5 m/s and turbulence intensity is less than 0.7 %. Fig. 3 illustrates the geometrical layout of the wind tunnel (e.g. Jang et al. 1997).

The measuring equipment used in this experiment is as follows:

· 6-component load cell : LMC-6524-10S (NEW)
· Hot wire anemometer : Model 1008 (KANOMAX)
· Digital micro manometer : DP-20A (Okano)
· Dynamic strain amplifier : DSA-100 (NEW)
· Low pass filter : 9B02 (NEC)
· Digital barometer : BN60705 (S.I.)

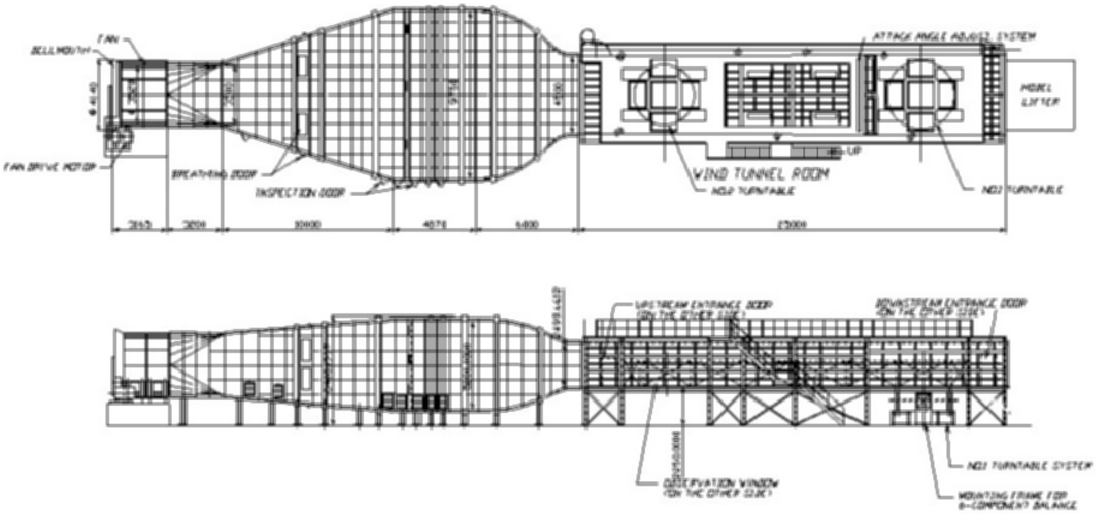

Fig. 3 Boundary layer wind tunnel.

· ADC : AT-MIO-16XE-50 (N.I.)

2.3 Experimental model

The wind tunnel test model used in this experiment is illustrated in Fig. 4, consisting of a 1/200 reduced scale model of a container crane type widely used in Korean berths. The original crane has a 50-ton lifting capacity, weighs 890 tons and has a 51 m outreach. The height of the girder from the ground is 40m and the height of the boom end tie in stowed mode can reach 100 m (e.g. Hanjin Heavy Industries & Construction Co. Ltd., 2000, HHIC). The scale model was constructed at Urban Architectural Models, a Korean manufacturer specialized in the production of architectural and wind tunnel test models. Two months were required to construct the model at a production cost of 5.5 million won. The material used for the scale model is balsa wood. In order to increase the natural frequency of the model, it was constructed to be light and stiff. To obtain reliable results of a wind tunnel test, not only the main structures of the container crane were constructed as a scale model but many detailed parts of the model, e.g. stairs, balustrade, etc, were also constructed. However, in the case of the girder, to analyze the effects of the wind loads according to the change of the machinery house location, the balustrade was eliminated in order to move the machinery house along the girder.

The machinery house comprises approximately 15% of the crane's total weight. Therefore, to evaluate the stability of a container crane according to the machinery house location, we installed a representative machinery house to examine three specific cases: Case 3: D=6 m (30 mm in model); Case 2: D=13 m (65 mm in model); and, Case 1: D=33 m (165 mm in model), where D represents the distance of the machinery house from the intersecting point of the girder, the boom, and the leg.

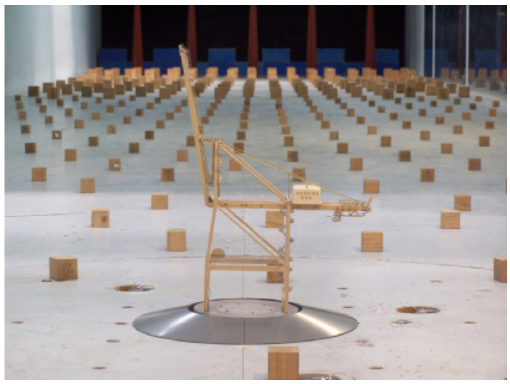

Fig. 4. The container crane model used for the wind tunnel test.

2.4 Experimental Process

The experimental process is described as follows. Firstly, in the wind tunnel the boundary layer was simulated to represent the designed wind velocity of

75 m/s (fastest velocity) and the shoreline terrain roughness category. The reduced scale (1/200) model of a container crane was installed on top of a 6-component load cell. Subsequently, each directional drag and overturning moment coefficient was measured with respect to the change in the incidence angle of the wind load from Case 1, in which the machinery house is located outside the land-side leg. At this point, the data were measured at 10-degree intervals, from 0-degrees to 180-degrees, because a container crane is a symmetrical model.

In the alternative cases, in which the machinery house was moved to the sea-side leg, wind load coefficients were measured by the same experimental process. Using these results, the wind load and overturning moment applied to a container crane and the uplift forces at each supporting point were calculated.

Figure 5 presents the flow chart for the wind tunnel test of the container crane model, and the definition of the incidence angle of the wind load is shown in Fig. 6.

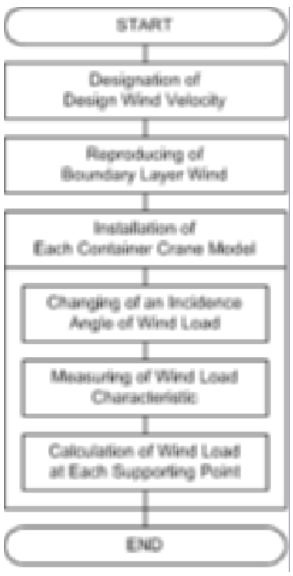

Fig. 5. Flow chart of the wind tunnel test of the container crane

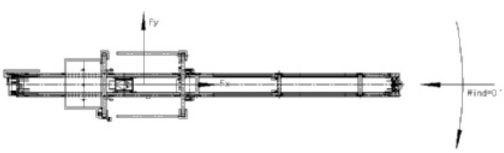

Fig. 6. Definition of incidence angle of wind load.

Data acquisition conditions for this experiment consist of the following parameters:

· Model scale : 1/200
· Wind velocity scale : 1/13.3
  - Design wind velocity : 75 m/s (at 64 m height)
  - Wind tunnel test velocity : 5.6 m/s (at 32 cm height)
· Time scale : 1/15
  - Actual time : 600 sec
  - Wind tunnel test time : 40 sec
· Scaling frequency : 120 Hz
· Number of measurements : 10 times
· Total number of data : 120 Hz×40 sec×10 times = 48,000 EA / ch

3. Results and discussions

3.1 Mean wind load coefficients

Using Eqs. (1)~(4), each directional drag and overturning moment coefficient was computed,

$$C_{Fx} = \overline{F_x} / (q_H BH) \quad (1)$$

$$C_{Fy} = \overline{F_y} / (q_H DH) \quad (2)$$

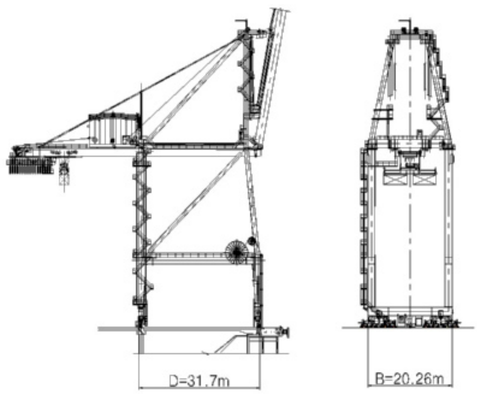

Fig. 7. Representational length of the container crane.

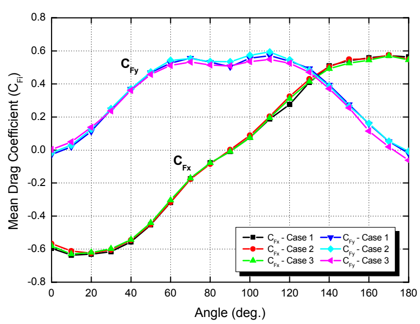

Fig. 8. Mean drag coefficient according to incidence angle of wind load.

$$C_{Mx} = \overline{M_x}/(q_H DH^2) \quad (3)$$

$$C_{My} = \overline{M_y}/(q_H BH^2) \quad (4)$$

where, B and D are the representational lengths of the container crane shown in Fig. 7, H is the height of the container crane (64 m), and q_H is the standard wind pressure.

Figures 8 and 9 present the drag and overturning moment coefficients obtained using the wind tunnel test. Coefficients obtained at 0°, 90°, 180° and the maximum values of those coefficients are presented in Table 1.

In the case of X-directional drag coefficients, those at an incidence angle of 10°~20° are 6.9% (case 1), 10 % (case 2), and 8.6 % (case 3) larger than those at 0° for each case. Case 1, 2, and 3 are the parameters to evaluate the structural stability of a container crane according to the machinery house location. For the Y-directional drag coefficients, the maximum values occurred at an incidence angle of 110°. The coefficients for an incidence angle of 110° are 13.5 % (case 1), 9.9 % (case 2), and 7.2 % (case 3) larger than those measured at an incidence angle of 90° in each case. However, the variation of the X and Y directional drag coefficients according to each case were almost the same at any incidence angle.

Table 1. Wind load coefficients according to each case.

Case		0°	90°	180°	Max
Case 1	C_{Fx}	-0.5951	-0.0093	0.5630	-0.6363
	C_{Fy}	-0.0272	0.5038	-0.0212	0.5720
	C_{Mx}	0.0154	-0.2379	0.0001	-0.2842
	C_{My}	-0.5433	0.0159	0.5241	-0.5886
Case 2	C_{Fx}	-0.5673	0.0015	0.5480	-0.6243
	C_{Fy}	-0.0162	0.5341	-0.0084	0.5930
	C_{Mx}	0.0017	-0.2469	0.0071	-0.2847
	C_{My}	-0.5628	0.0291	0.5172	-0.6161
Case 3	C_{Fx}	-0.5799	-0.0085	0.5447	-0.6298
	C_{Fy}	0.0019	0.5091	-0.0626	0.5485
	C_{Mx}	0.0001	-0.2377	-0.0145	-0.2737
	C_{My}	-0.5623	0.0167	0.6508	0.6508

In the case of the X-directional overturning moment coefficients, the maximum values were -0.2942 (case 1), -0.2847 (case 2), and -0.2737 (case 3) at incidence angles between 110°~120°, but the Y-directional maximum overturning moment coefficient values for each case were twice as large as those for the X-direction. The Y-directional maximum values for each case were -0.5886 (20°), -0.6161 (40°), and 0.6508 (180°).

The variation of X and Y directional overturning moment coefficients with respect to the change of the machinery house location were almost the same, like a distribution of drag coefficients at any angle. However, in the case of the Y-direction, results with comparatively large variations occurred at some angles. This was due to an error which occurred in the wind tunnel test. In this test, in order to minimize the resonance effect, the test model was constructed having an increased natural frequency resulting from the use of balsa wood whose mechanical characteristics are light-weight yet stiff. But, the scale model

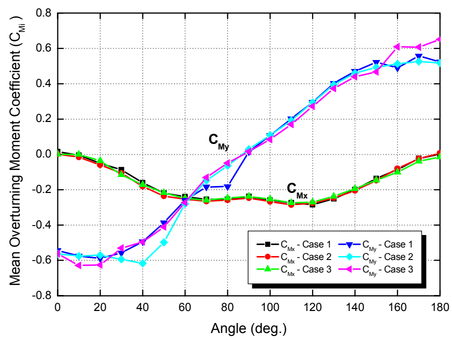

Fig. 9. Mean overturning moment coefficient according to incidence angle of wind load.

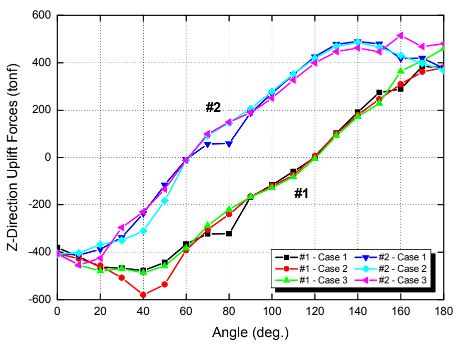

Fig. 10. Uplift forces of #1 and #2 supporting points according to incidence angle of wind load.

vibrated easily because the geometrical characteristics of members of the container crane were constructed to be slender and long. We concluded that the error was induced by the vibration due to the geometrical characteristics of the test model.

The distribution of the drag coefficient according to the wind load direction was compared with that of the overturning moment coefficient; they were determined to have a nearly identical distribution at any angle. The incidence angle of the wind load at which the maximum value of each coefficient occurred was not found at 0° or 90° with respect to the container crane, but at 10° ~ 20°. Generally, because the wind load is computed for the X (0°) and Y (90°) directions at the container crane design stage, compensational factors should be applied to the container crane design in order to consider an inclined wind load effect.

3.2 Uplift forces at supporting points

Figures 10 and 11 illustrate the uplift forces at each supporting point according to the incidence angle of the wind load. These uplift forces were induced by the wind load. The weight of the container crane was not considered. The position and description of each supporting point of the container crane is shown in Fig. 12. Because the container crane has a symmetrical shape, the uplift forces of #1 and #2 were equal to those of #3 and #4, but their directions were opposite. Because the uplift forces obtained by the wind tunnel test did not take into consideration the weight of the container crane, they demonstrated nearly the same value for every location of the machinery house.

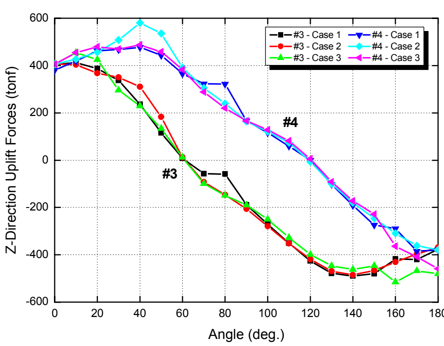

Fig. 11. Uplift forces of #3 and #4 supporting points according to incidence angle of wind load.

According to the result of the wind tunnel test, if the incidence angle of the wind load was 20°~ 40° or 130°~150°, high uplift forces reaching 490tonf occurred at the supporting points denoted #2 and #4. However, in the case of an actual container crane, these forces would be reduced by opposing compressive forces produced by the weight of the container crane. Therefore, in order to analyze the uplift force at the supporting point we considered the uplift force at each supporting point using the wind tunnel test and the compressive force due to the weight of the container crane.

The container crane used in this study has a heavy body weighing as much as 890tonf. The uplift forces exerted at each supporting point differ from the wind tunnel test results if the weight of the container crane is considered. In Case 1, in which the machinery house was located outside the land-side leg, the compressive forces at each supporting point due to the weight of the container crane are shown in Table 2 (e.g. Lee et al., 2005).

Figure 13 presents the results for Case 1, considering simultaneously the uplift forces obtained

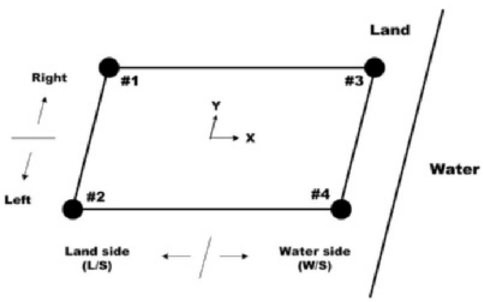

Fig. 12. Supporting point ID and position of the container crane.

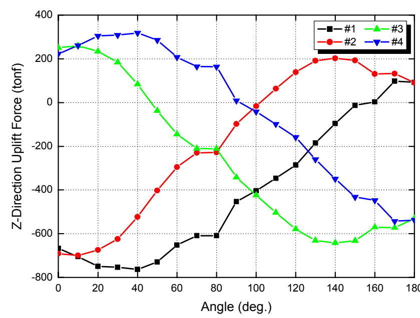

Fig. 13. Actual uplift forces at each supporting point, considering the weight of a container crane.

Table 2. Compressive forces at each supporting point caused by the weight of the container crane.

Supporting Point	#1	#2	#3	#4
Compressive Force	286.7 tonf	287.0 tonf	152.8 tonf	158.0 tonf

using the wind tunnel test and the actual weight of the container crane obtained from Table 2. In this figure, we confirmed that uplift forces were offset by container crane weight. The maximum actual uplift force was 320tonf at supporting point #4 when the incidence angle was 20° ~ 40°.

The compressive forces are presented in Table 2. For Case 1, in which the machinery house is located outside the land-side leg, and for Cases 2 and 3 in which the machinery house is moved toward the sea-side leg, we conclude that the compressive forces at points #1 and #2 will decrease but those at points #3 and #4 will increase because of the movement of the center of gravity.

4. Conclusions

In this manuscript, by analyzing the effects of wind loads on the stability of a 50-ton container crane using a wind tunnel test, we determined each directional drag and overturning moment coefficient according to incidence angle and the estimation method for uplift forces at each supporting point of the crane under wind load. Designers can use these data for improving the wind resistance of container cranes.

In the future, we propose to perform finite element analysis for each case in order to develop an improved type of container crane. Using the wind load coefficients derived in this study and comparing the results using finite element analysis with wind tunnel test results, the stowing devices and stowed configuration of future container cranes may be designed more precisely because the uplift forces affecting them can be more accurately calculated.

Acknowledgement

This work was supported by the National Research Laboratory Program of the Korean Ministry of Science and Technology (MOST).

References

Han, G. J., Lee, H., Shim, J. J., Han, D. S., Ahn, C. W., Jeon, Y. H., 2004, "Study on the Wedge Angle of Wedge Type Rail Clamp for Container Crane," *J. KSPE*, Vol. 21, No. 9, pp. 119~126.

Hanjin Heavy Industries & Construction Co. Ltd., 2000, "Structural & Mechanical Calculation for 50-Ton Container Crane for Pusan Port"

Jang, H. S., Kim, Y. S., Hwang, K. S., 1997, "Introduction of Wind Tunnel Laboratory in Hyundai Institute of Construction Technology," *J. WEIK*, Vol. 1, No. 1, pp. 58~65.

Kang, S. H., Lee, D. H., Cho, K. J., Choi, S. H., Huh, J., 1988, "Experimental Studies on the Estimation of Wind-Load of a Container Crane and Its Development," *J. KSME*, Vol. 12, No. 4, pp. 892~899.

Lee, S. W., Shim, J. J., Han, D. S., Park, J. S., Han, G. J., Lee, K. S., Kim, T. H., 2005, "The Effect of Wind Load on the Stability of a Container Crane," *J. KSPE*, Vol. 22, No. 2, pp. 148~155.

Ministry of Construction & Transportation of the Korean Government, 2000, "Design Criteria of a Road Bridge"

Ministry of Construction & Transportation of the Korean Government, 2000, "Load Criteria of Building Structures."